

Ground Level Enhancement Events of Solar Cycle 23

N Gopalswamy¹, H Xie², S Yashiro² & I Usoskin³

¹NASA Goddard Space Flight Center, Code 695, Greenbelt, MD 20771, USA

²The Catholic University of America, Washington DC 20064, USA

³Sodankylä Geophysical Observatory, Oulu University, FIN-90014, Finland

Received 4 August 2008; accepted xx August 2008

Ground Level Enhancement (GLE) events, typically in the GeV energy range, are the most energetic of solar energetic particle (SEP) events that penetrate Earth's neutral atmosphere. During solar cycle 23, sixteen GLE events were observed with excellent data coverage of the associated solar eruptions. In this paper we examine the question of the source of these GLE particles using white light observations of coronal mass ejections, type II radio bursts, and soft X-ray flares. We show that the GLE events are consistent with shock acceleration in every single case. While we cannot rule out the possibility of the presence of a flare component during GLE events, we can definitely say that a shock component is present in all the GLE events. During the 2001 April 18 GLE event, the source was located ~30 degrees behind the west limb, which is too far away from the magnetic field lines connecting Earth and hence we can rule out the flare component. We also show the presence of interplanetary shocks using radio and in-situ observations.

Keywords: Ground level enhancement (GLE), Coronal mass ejection (CME), Flare, Shock, Solar energetic particle (SEP), Type II radio burst

PACS No.: 96.60.ph; 96.60.qe; 96.60.Vg; 96.50.Fm

1 Introduction

Ground level enhancement (GLE) events are solar energetic particle (SEP) events that reach the neutral atmosphere of Earth and produce secondary neutrons detected as sudden increases in cosmic ray intensity¹. The solar sources of the GLEs are energetic eruptions involving high-speed coronal mass ejections (CMEs) and intense solar flares. CMEs drive fast-mode MHD shocks, which accelerate electrons and ions. Particles are also accelerated in the reconnection region of the eruption. From imaging observations of hard X-rays and gamma rays² one can infer that the angular extent over which the flare particles propagate is very small (~foot-point separation of gamma-ray sources), while the CME-driven shock is much more extended. CME-driven shocks can also be inferred from metric and interplanetary (IP) type II radio bursts, which are also closely associated with SEP events^{3,4}. We use the GLE observations of solar cycle 23 to combine the CME, flare and type II burst observations and present a global view of the events. A preliminary report was published with 14 GLEs in the 2005 ICRC proceedings⁵. This paper presents the complete set of 16 GLEs with no more GLEs occurring as of mid 2008.

2 Observations

We use the list of GLE events made available on line at the Oulu Cosmic Ray station (<http://cosmicrays oulu.fi/GLE.html>). The Oulu Neutron Monitor is part of the World Neutron Monitor Network and has been obtaining cosmic ray data since 1964⁶. It detects neutrons at rigidity above ~0.8 GV (the local vertical geomagnetic cutoff rigidity). GLEs are identified as percentage of enhancement of the neutron monitor count above the background. During solar cycle 23, 16 GLE events were detected with intensities ranging from ~3% to 269%. The first event occurred on 1997 November 6, and the last event occurred on 2006 December 13. There was a slight increase in the number of GLE events as one progressed from the rise (4 GLEs), to the maximum (5 GLEs), and to the declining phases (7 GLEs). Thus, no solar cycle variation can be inferred from the occurrence rate, which seems to depend on the existence of super active regions on the Sun, which are prolific producers of CMEs⁷. For each GLE, we were able to identify a unique CME observed by the Solar and Heliospheric Observatory (SOHO) mission's Large Angle and Spectrometric Coronagraph (http://cdaw.gsfc.nasa.gov/CME_list).

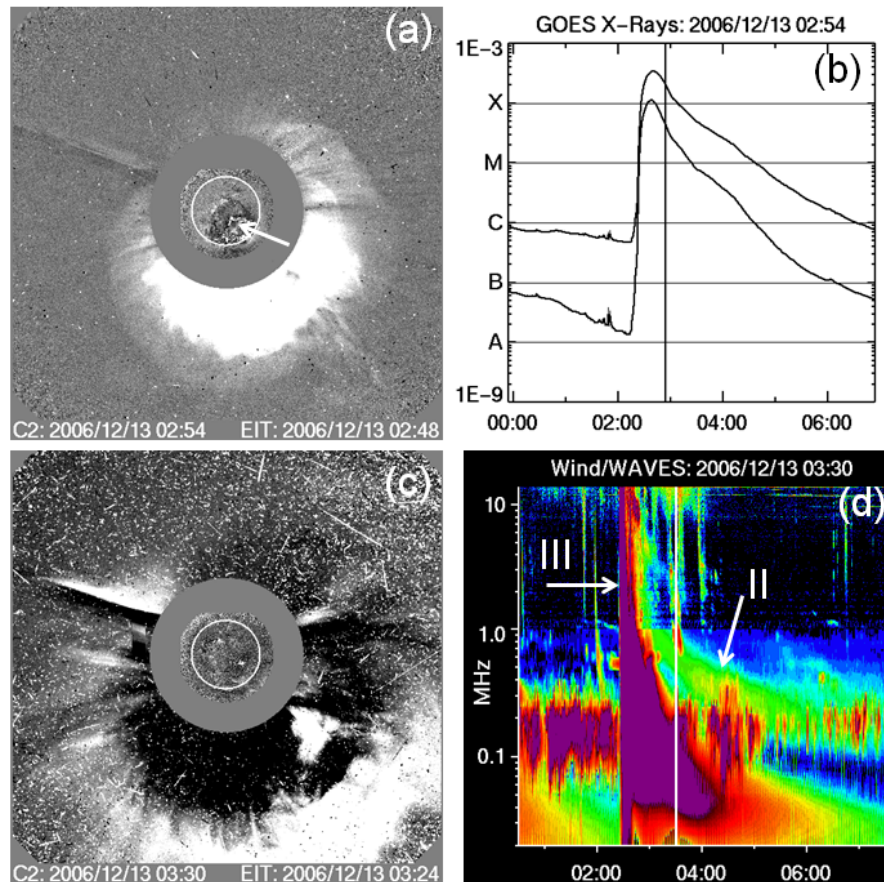


Fig 1 CME (a,c), soft X-ray flare (b), and interplanetary type II burst (d) associated with the 2006 December 13 GLE event. The CME can be seen in the SOHO/LASCO difference images at 02:54 and 03:30 UT with EIT difference images showing the disk activity. The approximate flare location is indicated by arrow. The vertical lines in the GOES plot and the Wind/WAVES dynamic spectrum mark the time of the corresponding LASCO frame on the left. The type II and type III bursts are marked by arrows in (d).

We also identify the source location of each CME based on the H-alpha flare location or from the EUV disturbances detected by the Extreme-ultraviolet Imaging Telescope (EIT) on board SOHO. Figure 1 shows the CME and flare associated with the GLE on 2006 December 13. The CME originated from the southwest quadrant (S06W23) in active region NOAA 0930 (pointed by arrow) and was a fast CME (1774 km/s) that evolved into a halo CME. In Fig.1b, one can see the EUV disturbance around the solar source region. Projection correction using a cone model⁸ yielded a speed of ~2164 km/s. The onset time of the CME is estimated to be ~02:25 UT after deprojection. Note that the image at 03:30 UT is already degraded

due to SEPs arriving at the SOHO spacecraft moments after its first appearance in the LASCO field of view (02:54 UT). The X3.4 flare started around 02:17 UT. The 8-minute delay of the CME may not be real because the CME was already at 5.3 solar radii when it first appeared, so the early acceleration phase was not observed. The Wind/WAVES radio dynamic spectrum (Fig.1d) shows that the type II burst started a few minutes after the type III burst (02:24 UT) at 14 MHz. However, the metric type II burst started as early as 02:26 UT (Solar Geophysical Data). The IP type II burst continued down to ~150 kHz before fading, but the shock was well observed in the Thermal Noise Receiver (TNR) dynamic spectrum at

~13:55 UT on December 14. The shock arrival at 1 AU was also marked by an energetic storm particle (ESP) event, which is an enhancement of locally accelerated particles detected as the shock spacecraft. The GLE itself was detected at 02:45 UT by the Oulu neutron monitor and the intensity peaked at 03:05 UT. The release time of the GLE particles at the Sun is calculated assuming a magnetic field line length of 1.2 AU. It takes ~11 min for ~1 GeV particles to travel this distance. To make it easier to compare, we subtract ~8 min for the light travel time to 1 AU (so as to be on par with the arrival of electromagnetic signals at 1 AU)⁹. This makes the GLE release time at the Sun as 02:42 UT. Clearly, both the flare and CME started well before the time of release of the GLE particles at the Sun. We followed this procedure to gather information for all the GLE events of cycle 23.

There was no LASCO data for the GLE event of 1998 August 24 because SOHO was temporarily disabled around that time. However, there was an IP type II that lasted all the way to the local plasma frequency at Wind/WAVES, which means there should have been a powerful CME associated with this event. Solar wind plasma and magnetic field data clearly show CME material, so we confirm the existence of a CME. For the GLE on 2001 April 18, the flare occurred behind the west limb, so there is no

flare information. However, the active region is estimated to be ~30° behind the limb, based on its location on the disk before rotating behind the limb. The CME was well observed from above the southwest limb. Observations in X-rays, microwaves, and EUV all show that the source was behind the southwest limb¹⁰. The same active region produced another GLE event on April 15 when the active region was at S20W85.

Table 1 lists the 16 GLEs along with the properties of CMEs, flares, and radio bursts obtained as described above. The dates and Earth onset times of the GLEs are listed in columns 2 and 3. The solar release time (column 4) and peak time (column 5) of GLEs are normalized to the Earth-arrival times of electromagnetic signals. The percentage enhancement above background (GLE intensity), metric type II onset (column 7), decameter-hectometric (DH) type III onset (column 8), GOES X-ray flare onset (column 9), flare size with solar location (column 10), CME onset (column 11), CME height (in solar radii, Rs) at GLE onset (column 12), Sky-plane speed of CMEs (column 13), and the deprojected CME speed (column 14) are also listed. CME onsets were obtained by extrapolating the first appearance time in the LASCO FOV to the surface using the deprojected speed. The CME on 2005 January 20 was observed

Table 1 List of the 16 GLE events of solar cycle 23

Eve nt #	GLE event Date	GLE Onset (Obs)	GLE Onset (Inf)	Peak time (UT)	GLE Int. (%)	Type II Onset	Type III Onset	Flare onset	Flare Class /Location	CME Onset	CME ht (Rs)	Sky Speed (km/s)	Space Speed (km/s)
1	1997Nov06	12:10	12:07	14:00	11.3	11:53	11:52	11:49	X9.4/S18W63	11:39	5.2	1556	1726
2	1998May02	13:55	13:52	14:05	6.8	13:41	13:35	13:31	X1.1S15W15	13:32	3.3	938	1332
3	1998May06	08:25	08:22	09:30	4.2	08:03	08:01	07:58	X2.7/S11W65	07:55	3.8	1099	1208
4	1998Aug24	22:50	22:47	02:05	3.3	22:02	22:04	21:50	X1.0/N35E09	DG	DG	DG	DG
5	2000Jul14	10:30	10:27	11:00	29.3	10:28	10:18	10:03	X5.7/N22W07	10:25	1.4	1674	1741
6	2001Apr15	14:00	13:57	14:35	56.7	13:47	13:49	13:19	X14/S20W85	13:35	3.3	1199	1203
7	2001Apr18	02:35	02:32	03:10	13.8	02:17	02:15	02:11	?/S23W117	02:11	5.9	2465	2712
8	2001Nov04	17:00	16:57	17:20	3.3	16:10	16:13	16:03	X1.0/N06W18	16:13	8.0	1810	1846
9	2001Dec26	05:30	05:27	06:10	7.2	05:12	05:13	04:32	M7.1/N08W54	05:06	4.2	1446	1779
10	2002Aug24	01:18	01:15	01:35	5.1	01:01	01:01	00:49	X3.1/S02W81	00:59	3.6	1913	1937
11	2003Oct28	11:22	11:19	11:51	12.4	11:02	11:03	11:00	X17/S20E02	11:07	3.9	2459	2754
12	2003Oct29	21:30	21:27	00:42	8.1	20:42	20:41	20:37	X10/S19W09	20:43	8.7	2029	2049
13	2003Nov02	17:30	17:27	17:55	7.0	17:14	17:16	17:03	X8.3/S18W59	17:19	3.0	2598	2981
14	2005Jan17	09:55	09:52	09:59	3.0	09:43	09:41	09:42	X3.8/N14W25	09:43	3.2	2547	2802
15	2005Jan20	06:51	06:48	07:00	277.3	06:44	06:45	06:39	X7.1/N14W61	06:33	4.0	3242	3675
16	2006Dec13	02:45	02:42	03:05	92.3	02:26	02:24	02:17	X3.4/S06W23	02:25	4.2	1774	2164

clearly only in one LASCO image, so we estimated the speed and onset by combining LASCO and EIT

data⁵. The sky-plane speed was ~3242 km/s, which becomes 3675 km/s, making the CME the fastest

among the GLE-associated CMEs. There were four groups of events that originated from the same active region: 2-3 from AR 8210, 6-7 from AR 9415, 11-13 from AR0486, and 14-15 from AR 0720.

3 Flare and CME properties

Table 1 shows that all the GLEs are associated with major soft X-ray flares. The smallest flare was M7.1 associated with the 2001 December 21 event (the only M-class event), while the largest one was the X17 flare on 2003 October 28. Figure 2 shows that the size distribution of flares associated with GLE events has a median value of X3.8, compared to just C1.6 for that of all flares of cycle 23. Another compilation of 38 GLE events from 1964 to 1991 by Kudela and co-workers¹¹ showed that the optical importance ranged from 1N to 3B for the associated H-alpha flares. Thus, the flares associated with GLEs are generally very powerful.

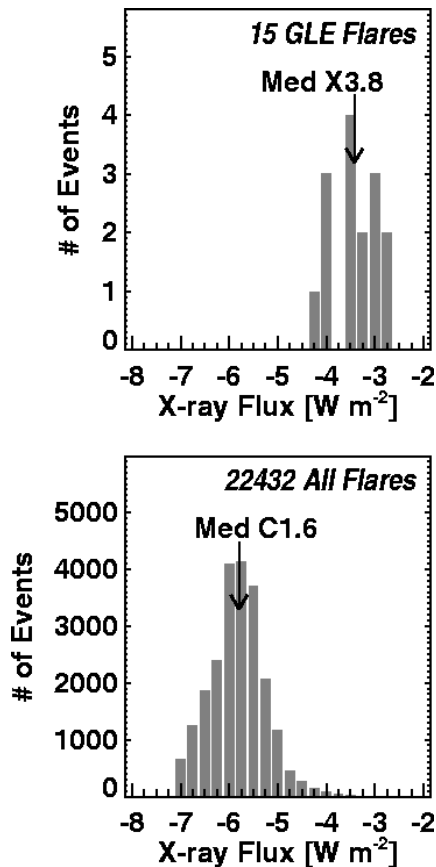


Fig. 2 Distribution of soft X-ray flare sizes for 15 GLE events (top) and all flares during the study period (bottom). The median values of the distributions are indicated by arrows.

The solar sources in Table 1 are generally located from the disk center to the west limb. In fact there were only 2 eastern events (E09 for 1998 August 24 event and E02 for the 2003 October 28 event) very close to the disk center. The fraction of eastern events is also very small (3 out of 38) in Kudela et al. compilation¹¹.

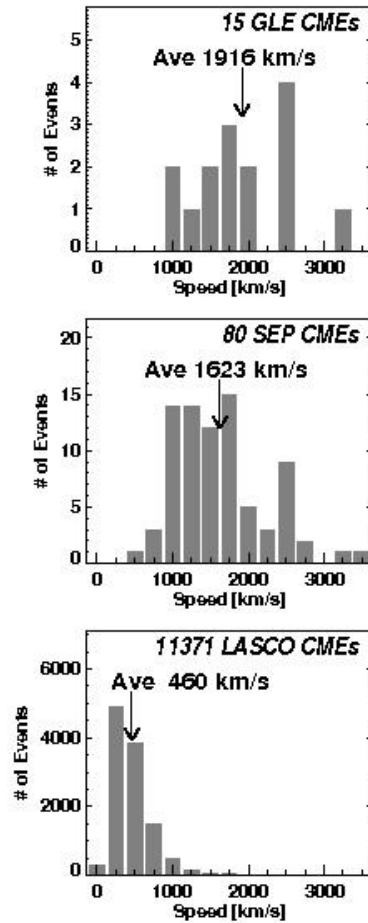


Fig. 3 CME speed distributions for GLE events (top), SEP events (middle), and all CMEs (bottom). The averages of the distributions are given on the plots.

The CME speed distributions (Fig. 3) show that the average speed of GLE associated CMEs (1916 km/s in the sky plane) is greater than that of the SEP associated CMEs (sky-plane speed ~ 1623 km/s). On the other hand, the GLE associated CMEs are more than 4 times faster than the average CME (460 km/s, which is the average of more than 11000 CMEs observed during the study period). In fact, the GLE associated CMEs constitute the fastest population of CMEs. It must be pointed out that the GLE events are a subset of the 80 SEP events shown in Fig. 3.

From Figs. 2 and 3 it is clear that energetic flares and CMEs accompany all the GLE events, which means both processes (shock and flare reconnection) are expected to contribute to the observed GLE. It is however difficult to separate these components. It is generally no problem in understanding the production of particles in the flare process from hard X-ray, microwave, and gamma-ray observations. These are due to downward propagating particles, which typically occupy a small angular extent. For example, in the largest GLE event of cycle 23 on 2005 January 20 the hard X-ray footpoints were separated by ~ 40 arcsec¹². Even the H-alpha flare ribbons (tip to tip) have an extent of only 225 arcsec, which corresponds to $13^{\circ}.6$ (heliographic). This is close to the size of flux tubes that connect the Sun and Earth. The widest dimension of the current sheet in which reconnection takes place and particles are accelerated cannot have an extent larger than this value. The gamma-ray footpoints are also separated by an extent similar to that of hard X-ray footpoints, although this could be slightly different². The outgoing particles may have a similar angular spread, which means flare particles maybe observed only for well-connected events. The principle is the same for impulsive SEP events, which originate from well-connected source regions. From this point of view, the 2005 January 20 GLE originated from N14W61, which is well connected. Some aspects of the GLE time profile such as a narrow peak with highly anisotropic particles¹³ may indicate flare particles, while bulk of the particles are due to shock acceleration. Clearly such cases are very rare because the 2005 January 20 event is the only one in cycle 23 that showed the anisotropic peak (H. Moraal, private communication). Two other GLE events had similar source location (1998 May 2 event from W65 and 2003 November 2 event from W59). Both of these events were weak by two orders of magnitude compared to the 2005 January 20 event. Three such GLE events in cycle 22 and one from cycle 19 were reported many years ago¹⁴, all well connected (W28 to W37).

If we exclude the spike component, all the GLE events are consistent with shock acceleration. Presence of fast and wide CMEs during each of the GLE event strongly indicates the existence of CME-driven shocks. The Alfvén speed in the corona at heights where type II radio bursts form is estimated to be in the range 400 – 1500 km/s¹⁵. Therefore, each

one of the CMEs is likely to be super-Alfvénic. The presence of a metric type II burst before the release of GLE particles also supports the existence of shocks in the corona. Finally, the presence of type II bursts at DH wavelengths indicates strong shocks, much stronger than cases where only metric type II bursts are present³. Table 2 shows the starting and ending times of DH type II bursts (columns 1-4) and their frequency extents (f1 – starting frequency and f2 – ending frequency in MHz). In most cases, the GLEs were released slightly before (3 to 33 min) the start of the DH type II burst and in a few cases slightly after (7 to 42 min). Note that in most cases the starting frequency is the highest observing frequency, which means we cannot tell at what frequency the burst really started. It can be anywhere up to the time of the metric type II burst. Most of the ending frequencies are below 0.1 MHz, which means the shocks were strong enough to produce electrons far into the interplanetary medium, often close to the observing spacecraft (at L1 point).

Table 2 Type II bursts in the Decameter-hecometric (DH) band from the Wind/WAVES Experiment

#	DH II Start		End		f1	f2
	Year	UT	Year	UT		
1	1997/11/06	12:20	11/07	08:30	14	0.1
2	1998/05/02	14:25	05/02	14:50	5 ^a	3.0
3	1998/05/06	08:25	05/06	08:35	14	5.0
4	1998/08/24	22:05	08/26	06:20	14	0.03
5	2000/07/14	10:30	07/15	14:30	14	0.08
6	2001/04/15	14:05	04/16	13:00	14	0.04
7	2001/04/18	02:55	04/18	14:00	1 ^b	0.10
8	2001/11/04	16:30	11/06	11:00	14	0.07
9	2001/12/26	05:20	12/27	05:00	14	0.15
10	2002/08/24	01:45	08/24	03:25	5	0.40
11	2003/10/28	11:10	10/29	24:00	14	0.04
12	2003/10/29	20:55	10/29	24:00	11	0.50
13	2003/11/02	17:30	11/03	01:00	12	0.25
14	2005/01/17	09:25	01/17	16:00	14	0.03
15	2005/01/20	07:15	01/20	16:30	14	0.03
16	2006/12/13	02:45	12/13	10:40	12	0.15

^aEarlier start possible f1 = 14 MHz at 14:06 UT; ^bType II like event starts 14 MHz around 2:30 UT

While one can understand that flare particles can flow both towards and away from the Sun, it is not clear if the shock particles produce any observable signature at the solar surface. One of the reasons is

the CME directly behind the shock, so the particles may not penetrate into the CME flux rope. The shock is also rapidly moving out (typically 1 Rs in 6 min). Therefore, it is more likely the shock particles move predominantly away from the Sun.

4 CME Height at GLE Release

Now we consider the CME location in the corona when the GLE particles are released. The heliocentric distance of the CME is simply referred to as CME height. After projection correction, we extrapolated the CME height at first appearance to the time of the GLE release using the speed corrected for projection effects. The CME height at the time of SEP release ranges from 1.4 to 8.7 Rs (Table 1). The distribution of CME heights at GLE release is compared with that at metric type II burst onset in Fig. 4. It is possible that the type II bursts originate from the flanks of the CME-driven shock, so the CME height represents the shock height only approximately. Nevertheless, the small CME height (1.6 Rs) at the time of metric type II burst means that CMEs have to travel an additional 2.8 Rs before releasing the GLE particles. Since the average speed of the GLE associated CMEs is ~ 2000 km/s, the CMEs have to travel an additional 15 min before the release. The CMEs are also expected to have finished acceleration reaching the highest speed when the GLE particles are released. Furthermore, the Alfvén speed in the corona also starts falling below its peak value around 3 Rs¹⁶. Therefore, the shock is likely to be the strongest around the time of the GLE release. If the anisotropic initial spike is from the flare site, the particles have to travel around the CME flux rope and pass through the CME-driven shock before arriving at Earth. Note also that the CME speed and the variation in Alfvén speed with height are immaterial for the flare particles, which typically are released at $\sim 20,000$ km above the solar surface. It is not clear how the shock affects the flare particles. It is possible that they are further accelerated by the shock before reaching the observer.

5 Delay Times

Figure 5 shows the delay of GLE release with respect to metric type II bursts, DH type III bursts, soft X-ray flares and CMEs. The median delay is the smallest for metric type II bursts (18 min) and the

largest for soft X-ray flares (27 min). The onset of DH type III bursts (delay = 19 min) is very close to

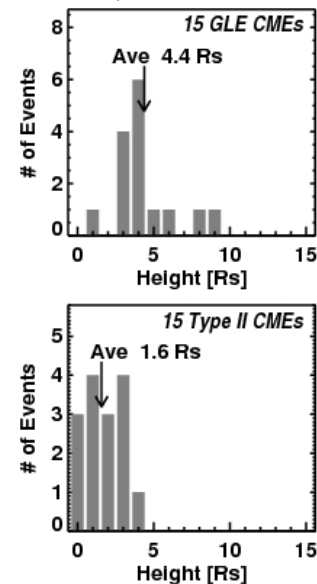


Figure 4 Distribution of CME height at the time of GLE release (top) and metric type II burst onset (bottom). The average values of the distribution are shown on the plots.

that of type IIs. The delay with respect to the CME onset (median 23 min) is intermediate. Thus particle acceleration by both shocks (evidenced by the type II bursts and flare reconnection (evidenced by type III bursts) seems to have started well before the GLE release. We may not be able to distinguish between the mechanisms from the delay time alone.

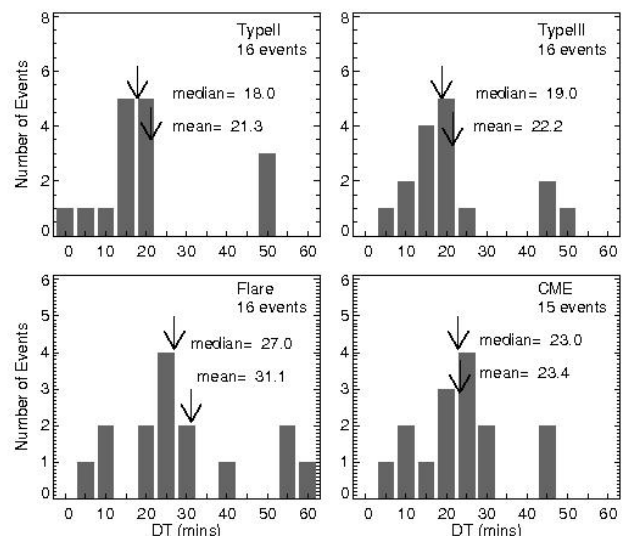


Figure 5 Delay of GLE release with respect to metric type II bursts, DH type III bursts, flares, and CMEs.

6 GLE Event of 2001 April 18

The GLE on 2001 April 18 is unique during solar cycle 23 in that the source location was $\sim 30^\circ$ behind the west limb. It is known for a long time that SEPs come from behind the west limb (see Fig. 6). In a recent study it was found that the SEP association of the behind the limb CMEs is similar to that of CMEs originating from $\sim W15$ considering the population of CMEs producing DH type II bursts¹⁷. A previous compilation of GLEs found that 9 GLE events (out of the 38) had their sources behind the west limb¹¹. During the current cycle the rate is much lower, because only one out of the 16 originated from behind the west limb. The 2001 April 18 CME was exceptionally fast (2465 km/s in sky plane and 2712 km/s deprojected). Given that high speed CMEs are generally associated with larger X-ray flares, one expects a large X-ray flare behind the limb. The event was in fact associated with an unusually large-disturbance above the limb recorded in X-rays, EUV, and microwaves¹⁰.

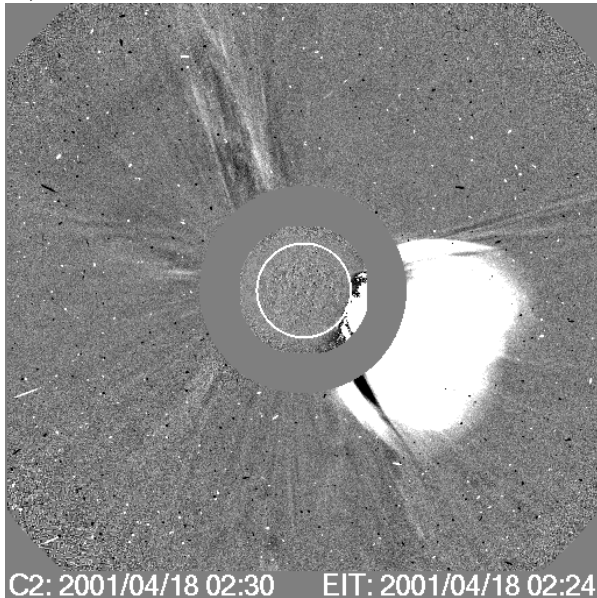


Figure 6 SOHO/LASCO C2 difference image with superposed EIT difference image showing the CME from behind the west limb. Note the EUV disturbance above the limb with nothing on the disk.

Backsided events like the 2001 April 18 event provide strong evidence for shock acceleration because the flare source has an angular extent of only $\sim 13^\circ$, which means it is very difficult for the flare particles to arrive at Earth from behind the limb. On the other hand CMEs are more extended

(width $> 60^\circ$), so the shock front is expected to cross the sky plane to the frontside. Similar argument applies to the poorly connected events erupting close to the disk center. It is highly likely that all the observed GLE particles are accelerated in the shock front in such events.

6 Summary and Conclusions

We analysed the GLE events of cycle 23, which is the first solar cycle that has extensive CME observations for almost all the GLEs. There were only 16 GLE events in cycle 23, clearly demonstrating that these are rare events with an occurrence rate of only ~ 1.5 per year. The number of GLE events does not follow the solar cycle, but steadily increases from the minimum to the declining phases. The GLEs arise mostly from super active regions (such as AR 0486) that produce many CMEs in quick succession. The GLEs are a small subset of large SEP events which total about 90 during cycle 23. Therefore, there is no surprise that the CME and flare properties of GLE events are similar to those of SEP events. In fact, the GLE associated CMEs are the fastest, the SEP associated CMEs being the second fastest. The flares are also very intense, being M7 or higher in X-ray importance (median X3.8). The CMEs are well under way by the time the GLEs are released (typically at a height of $\sim 4.4 R_s$) and have been driving shocks for at least 20 min. The solar eruptions associated with GLEs occur from near the disk center to locations well beyond the west limb. While it is difficult to tell the difference between flare and shock particles from the well-connected events, one can be sure of the shock particles for events from behind the limb. The same may be true of the poorly connected events from near the disk center. The extensive observations of flares and CMEs during the cycle 23 GLEs need to be further exploited for a better understanding of these rare events.

References

- 1 Meyer P. Parker E.N. & Simpson J.A. Solar cosmic rays of February 1956 and their propagation through interplanetary space, *Phys. Rev.*, 104 (1956) 768.
- 2 Lin R. P. et al., Particle Acceleration by the Sun: Electrons, Hard X-rays/Gamma-rays, *Space Sci. Rev.* 124 (2006) 233.
- 3 Gopalswamy N., Coronal Mass Ejections and Type II Radio Bursts, Geophysical Monograph Series - Volume 165: Solar Eruptions and Energetic Particles (American Geophysical Union, Washington DC), p 207.
- 4 Cliver E. W.; Kahler S. W. & Reames, D. V., Coronal Shocks and Solar Energetic Proton Events, *Astrophys. J.* 605

- (2004) 902.
- 5 Gopalswamy N., Xie H., Yashiro S. & Usoskin I., Coronal Mass Ejections and Ground Level Enhancements, Proc. 29th International Cosmic Ray Conference Pune (2005) 00, 101.
 - 6 Usoskin I. G. Mursula K., J. Kangas1 J. & Gvozdevsky G., On-Line Database of Cosmic Ray Intensities, Proceedings of ICRC 2001, p.1.
 - 7 Gopalswamy N., Yashiro S. & Akiyama, S., Coronal mass ejections and space weather due to extreme events, Proceedings of the ILWS Workshop. Goa, India. February 19-24, 2006, p.79.
 - 8 Xie H. Ofman & L. Lawrence G., Cone model for halo CMEs: Application to space weather forecasting, *J. Geophys. Res.* 109 (2004) A03109.
 - 9 Kahler S. W. Simnett G. M. & Reiner M. J., Onsets of Solar Cycle 23 Ground Level Events as Probes of Solar Energetic Particle Injections at the Sun, Proceedings of the 28th International Cosmic Ray Conference, 2003, p. 3415.
 - 10 Gopalswamy N., Radio Observations of Solar Eruptions, Solar Physics with the Nobeyama Radioheliograph, Proceedings of Nobeyama Symposium 2004, (Kiyosato, Japan, October 26- 29, 2004), Nobeyama Solar Radio Observatory, 2006, p.81.
 - 11 Kudela K., Shea M. A., Smart D. F. & Gentile L. C., Relativistic solar particle events recorded by the Lomnický štít Neutron Monitor, Proc. 1993 ICRC, 3 (1993) 71.
 - 12 Grechnev, V. V. et al., An Extreme Solar Event of 20 January 2005: Properties of the Flare and the Origin of Energetic Particles, *Solar Phys.* 2008 in press.
 - 13 Butikofer, R. Fluckiger E. O. Desorgher L. & Moser M.R., 20th European Cosmic Ray Symposium in Lisbon, Portugal, 2006.
 - 14 Shea M. A. & Smart D. F. Unusual Intensity-Time Profiles of Ground-Level Solar Proton Events, AIP Conference Proceedings, Vol. 374. Woodbury, NY: American Institute of Physics, 1996, p.131.
 - 15 Gopalswamy N. et al., Radio-Quiet Fast and Wide Coronal Mass Ejections, *Astrophys. J.* 674 (2008) 560.
 - 16 Gopalswamy N., et al., Coronal Mass Ejections, Type II Radio Bursts, and Solar Energetic Particle Events in the SOHO Era, *Ann. Geophysicae*, in press.
 - 17 Gopalswamy N., Lara A., Kaiser M. L. & Bougeret J. L., Near-Sun and near-Earth manifestations of solar eruptions, *J. Geophys. Res.* 106 (2001) 25261.